electronics

Article

Global Maximum Power Point Tracking of Photovoltaic Module Arrays Based on an Improved Intelligent Bat Algorithm

Kuei-Hsiang Chao * and Thi Thanh Truc Bau

Department of Electrical Engineering, National Chin-Yi University of Technology, Taichung 41170, Taiwan; s4b112128@student.ncut.edu.tw
* Correspondence: chaokh@ncut.edu.tw; Tel.: +886-4-2392-4505 (ext. 7272); Fax: +886-4-2392-2156

Abstract: In this paper, a method based on an improved intelligent bat algorithm (IIBA) in cooperation with a voltage and current sensor was applied in maximum power point tracking (MPPT) for a photovoltaic module array (PVMA), where the power generation performance of a PVMA was enhanced. Due to the partial shading of the PVMA from climate changes or the surrounding environment, multiple peak values were generated on the power–voltage (P-V) curve, where the conventional MPPT technology could only track the local maximum power point (LMPP), hence the reduction in output power of PVMAs. Therefore, the IIBA-based MPPT was proposed in this paper to solve such issues and to ensure the capability of a PVMA in tracking the global maximum power point (GMPP) and utilization for enhancing the output power of a PVMA. Firstly, the Matlab/Simulink software was used to establish a boost converter model that simulated the actual 4-series–3-parallel PVMA under different shaded conditions, where the P-V curve with 1-peak, 2-peak, 3-peak and 4-peak values were generated. Subsequently, the tracking paces of the conventional bat algorithm (BA) were adjusted according to the gradient of the P-V curve for a PVMA. At the same time, 0.8 times the maximum power point (MPP) voltage V_{mp} under standard test conditions (STCs) for a PVMA was set as the initial tracking voltage. Lastly, the simulation results proved that under different environmental impacts, the proposed IIBA led to better performances in tracking both dynamic and steady responses.

Keywords: improved intelligent bat algorithm; P-V curve; partial shaded condition; maximum power point tracking; global maximum power point

check for updates

Citation: Chao, K.-H.; Bau, T.T.T. Global Maximum Power Point Tracking of Photovoltaic Module Arrays Based on an Improved Intelligent Bat Algorithm. *Electronics* **2024**, *13*, 1207. https://doi.org/10.3390/electronics13071207

Academic Editor: Rui Castro

Received: 26 December 2023
Revised: 10 March 2024
Accepted: 15 March 2024
Published: 25 March 2024

1. Introduction

The photovoltaic system mainly consists of the photovoltaic module array (PVMA), inverter, transmission and distribution system. Among them, the inverter also provides the function of maximum power point tracking (MPPT) [1–4]. Since the output power of a PVMA differed along with changes in magnitude of solar irradiance and temperature, control with an MPPT controller is needed, so the PVMA could produce the maximum power despite any solar irradiance or temperature.

Since the PVMA would generate a correspondent P-V curve under different ambient temperature and solar irradiance, common conventional MPPT technology included the voltage feedback method, constant voltage method [5], power feedback method [6], perturbation and observation (P&O) method [7] and incremental conductance (INC) method [8]. However, although these conventional methods could track maximum power point (MPP) when a PVMA functions normally, once partial shading or faults occur in the PVMA and produce a P-V curve with multi-peak values, the global maximum power point (GMPP) might not be tracked, where only the local maximum power point (LMPP) could be tracked.

In recent years, to solve multiple peak values generated from the P-V curve due to certain modules in a PVMA being shaded, where conventional MPPT methods became invalid, many smart MPPT methods were proposed [9–23]. These methods included the cuckoo search algorithm (CSA) [9–11], cat swarm optimization (CSO) [12–14], genetic algorithm (GA) [15–17], teaching–learning-based optimization (TLBO) [18], grey wolf algorithm [19,20] and bat algorithm (BA) [21–23]; however, each algorithm had its unique strengths and constraints. Among them, CSA [9–11] was a global search algorithm inspired by bird behavior of food searching. Such an algorithm had the strength of global searching, where an understanding of system characteristics in advance was not required but helped to allocate the true optimal values. In addition, such a method was self-adaptive and capable of accommodating with the ever-changing environment and weather conditions, which further enhanced the power generation efficiency of the photovoltaic power generation system. Although the principle of CSA was more intuitive and relatively simple to realize, the parameter adjustment demanded precise implementation to ensure optimal searching performance. Therefore, the converging speed might be slower under certain circumstances. CSO [12–14] was an algorithm inspired by a cat swarm capturing prey, which provided good tracking performance when applied in MPPT. Such algorithm also had the characteristic of global searching that was helpful to allocate the optimal working point, where understanding of system characteristics in advance was not required either, but capable of accommodating the ever-changing environmental conditions. However, the parameter adjustment of CSA demanded precise implementation to realize optimal searching performance. Moreover, due to its randomness in searching, different search results might be obtained from selection of different iteration parameters. In addition, the GA [15–17] adopted the genetic process in nature as inspiration; through operations of generic selection, crossover and mutation, there were certain strengths in MPPT. Such an algorithm was capable of global searching and optimization, which could help to allocate the optimal working point of the system with flexibility; therefore, the parameter adjustment could be implemented according to different system requirements and environments. However, the calculation cost of the GA was higher; within large or complex systems in particular, a longer calculation time might be needed, which affected the system promptness. Furthermore, the GA required precise parameter adjustments and the risk of being stuck in the local maximum did exist, thus system requirements for parameter optimization should be considered prior to applying a GA in MPPT for a PVMA so effective tracking to the GMPP could be ensured. TLBO [18] was a global optimization algorithm developed from teaching and learning concepts, which had been applied in MPPT for a PVMA extensively. One of the strengths for a TLBO was its capability of global searching, which allowed the allocation of an optimal working point for a PVMA without the requirement of understanding system characteristics in advance. Through the teaching and learning concepts, the algorithm could continuously optimize solutions, which enhanced the performances in converging speed and global optimization. Moreover, the principle of the TLBO was easy to comprehend and relatively easy to realize, which made it an optimization tool that was extensively applied. However, there were certain constraints on the TLBO; similar to other algorithms, precise parameter adjustments were also needed to realize the optimal performance. Furthermore, due to the randomness, the tracking results might also differ due to the selection of different parameters. Therefore, suitable iteration parameters could only be selected through multiple tests so that steady tracking performance could be ensured. Although the grey wolf algorithm [19,20] provided merits such as a simple architecture and less parameters required during the procedure of search optimization, the disadvantages included the possibility of eventually being stuck in the local optimum, poor accuracy and slow convergence. The BA [21–23] on the other hand was inspired by bats searching for food and was applied in MPPT for a PVMA. The BA had the characteristics of global searching and random searching, where the randomness allowed allocating a new MPP under different environmental conditions, hence the enhancement in fitness level. Furthermore, since the work principles of the BA were easy to comprehend, it was relatively easy to realize. However, precise parameter adjustment was still needed and there was higher sensitivity on the initial conditions, which might possibly lead to the tracking of different MPPs under a limited iteration quantity. At the same time, the BA was constrained by a maximum bat flying speed and minimum pulse rate that needed to be defined, which might affect the tracking performances. In summary, all these intelligent algorithms could provide MPPT for a PVMA, yet detailed assessments on their strengths and weaknesses were required, where suitable iteration parameters were further selected to ensure better tracking performance.

Based on the reasons given above for enhancing the performance of a photovoltaic power generation system and realizing better efficiency in energy conversion, the IIBA was proposed in this paper, which was applied in MPPT when multiple peak values occurred in P-V curves with a PVMA under partial shading, so the GMPP could be tracked swiftly and, in turn, provide better performance in steady and dynamic responses compared to the conventional BA. In [24] the author first searched for the maximum power point (MPP) using the intelligent bee colony algorithm. Then, using traditional P&O algorithms, the next tracking direction was validated to track the global maximum point. However, in this study, search and tracking were performed concurrently, and the direction did not require the use of other algorithms. As a result, the algorithms in this paper reduced the system's overall calculation load, shortening tracking time. In [25] the author adopted the gradient of the P-V curve to modify traditional firefly algorithms. However, in his paper, the author adjusted the tracking pace by dividing the work interval of the P-V curve. The individual locations were then adjusted based on the tracking pace.

In this paper, two types of improved bat algorithms (IBA) are proposed. In particular, the gradient of the P-V curve is used to regulate the tracking pace while also fixing the beginning tracking voltage at 0.8 times the maximum power voltage V_{mp} (V_{st} = 0.8 V_{mp}). The improved bat algorithm not only improves tracking response speed over traditional bat algorithms, but it also reduces power loss during the tracking process, increasing power generation efficiency. Simultaneously, it can reduce the amplitude of the oscillation nearby in a back-and-forth motion while tracking the global maximum power point, thereby improving tracking performance in the steady state.

This paper's content is organized as follows: in the second section, the characteristics of the photovoltaic module array are introduced; in the third section, the working principles of traditional bat algorithms and the overall system framework of their application in photovoltaic module arrays to accomplish maximum power point tracking are explained; in the fourth section, the improved bat algorithms are proposed to solve the drawbacks of applying the traditional bat algorithm to the photovoltaic module; the fifth section uses simulation results to validate the tracking performance of the proposed improved bat algorithm; finally, the sixth section draws conclusions and explains this paper's contributions and future research directions.

2. Characteristics of a PVMA

In the case of partial modules of a PVMA under different shading situations, multiple peak values would occur on the P-V curves. Therefore, MATLAB R2022a/Simulink [26,27] was applied to build the PVMA model, which adopted SWM-20W photovoltaic modules produced by MPPTSUN Co. Ltd. (DongGuan, Guangdong Province, China) to form the test cases with a 4-serial–3-parallel module array, and the specifications for the single module are shown in Table 1 [28]. Figures 1 and 2 display the P-V and I-V curves derived from the simulation with a 4-serial–3-parallel PVMA under STCs (i.e., solar irradiance at 1000 W/m^2, temperature at 25 °C and AM (air mass) at 1.5), where all modules were not shaded at all and the third photovoltaic module in the first series was under 50% shading. From Figure 2, it can be observed that with a single module in a certain series under shading, 2-peak values would be generated on the P-V curve, where the traditional MPPT could only track the LMPP instead of the GMPP.

Table 1. Specifications of single SWM20W photovoltaic module [28].

Electric Parameter	Specifications
Voltage of open circuit (V_{oc})	22.32 V
Current of short circuit (I_{sc})	1.15 A
Voltage of maximum power point (V_{mp})	18.18 V
Current of maximum power point (I_{mp})	1.10 A
Power at maximum power point (P_{mp})	20.00 W

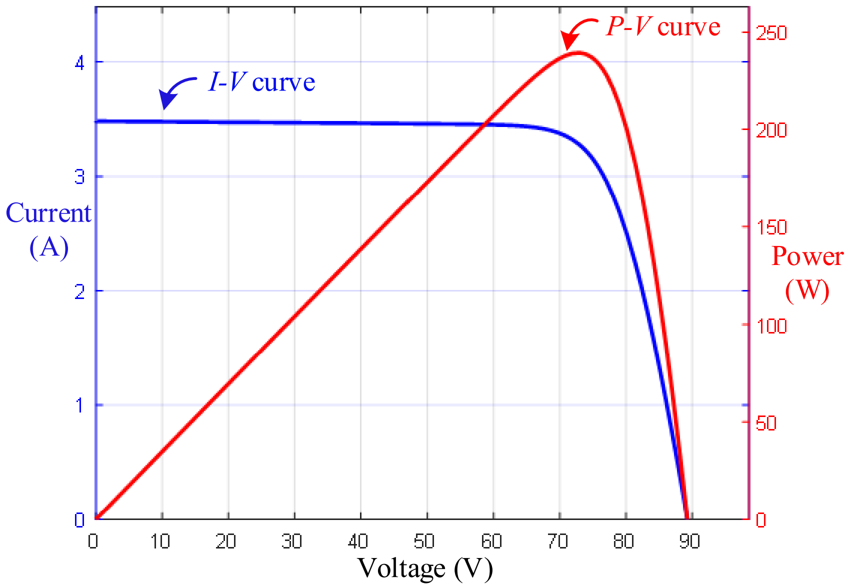

Figure 1. P-V and I-V curves derived from simulation for a PVMA under STCs.

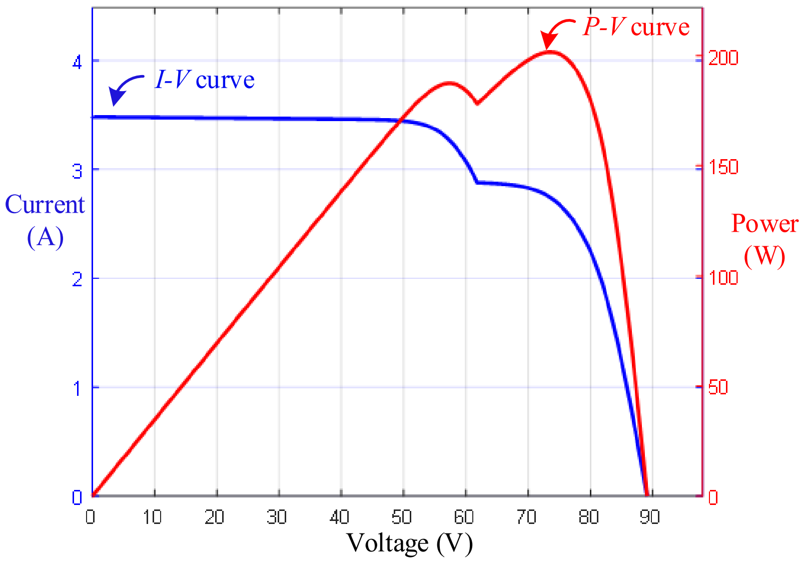

Figure 2. P-V and I-V curves derived from simulation with 1 module under 50% shading for a PVMA.

3. MPPT Architecture of a PVMA

Figure 3 illustrates the MPPT architecture proposed in this paper, which included two sub-systems: namely, (1) a boost converter and (2) an MPPT controller with the IIBA. During the actual tests, the feedback of the PVMA voltage and current was conducted via a differential amplifier. A TMS320F2809 digital signal processor (DSP) (Texas Instruments, Dallas, TX, USA) was adopted to realize the IIBA, where the conduction and cut-off time of switch S were controlled in MPPT for a PVMA.

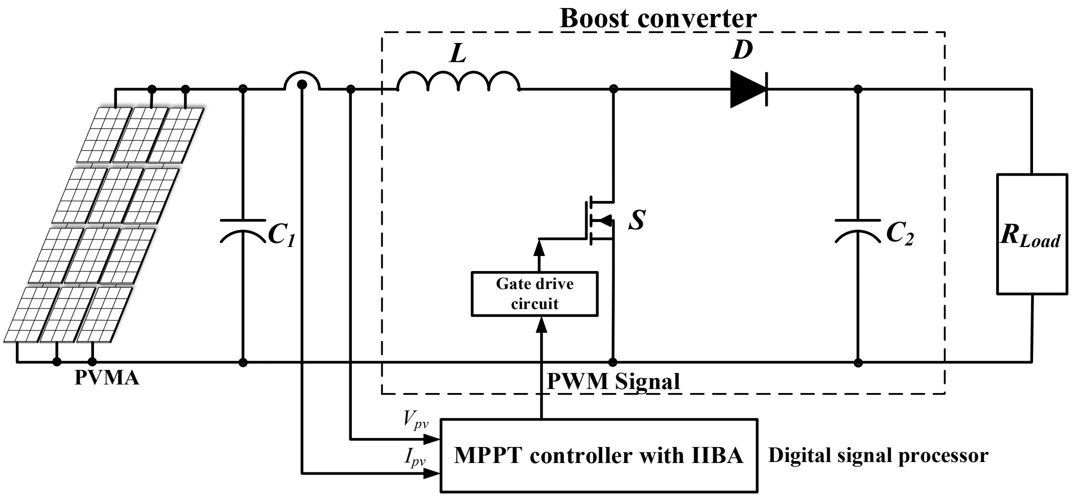

Figure 3. MPPT structure of a PVMA.

3.1. Work Principles for Boost Converter

Figure 4 displays the main circuits of the boost converter [29], where the circuit structure consisted of a switch, a fast diode, a storage inductor and a filter capacitor. The switch conduction and cut-off was controlled via pulse width modulation (PWM); the switching period of the converter was T; the switch conduction time was DT; the switch cut-off time was (1-D)T. Among them, D was the duty cycle defined as $D \triangleq \frac{t_{\text{on}}}{T}$, while t_{on} was the switch conduction time within one cycle. With the assumption that the inductor current operated in continuous conduction mode under extensive capacitance, the output voltage V_o would be a fixed value. The relationship between output voltage V_o and input voltage of the boost converter is shown as Equation (1) [29]. Due to $0 \leq D \leq 1$, $V_s \leq V_o \leq \infty$ was derived accordingly, and the converter served as a boost converter.

$$V_o = \frac{V_s}{1 - D} \tag{1}$$

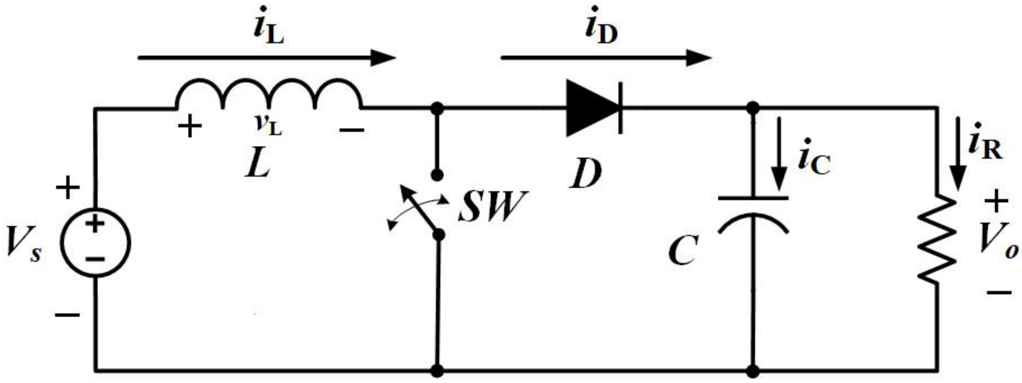

Figure 4. Main circuit structure of boost converter.

Should the boost converter operate at a higher switch frequency, the volume of the storage inductor and filter capacitor could be reduced [29]. As a result, 25 kHz was applied in this paper as the switch frequency for the boost converter. Table 2 lists the component specifications of the boost converter adopted in this paper.

Table 2. Component specifications of boost converter.

Component	Specifications
Filter capacitor C_1	220 µF/400 V
Filter capacitor C_2	470 µF/500 V
Storage inductor L	1.66 mH/7.5 A
Fast diode D Diode IQBE60E60A1	600 V/60 A
Switch S MOSFET IRF460	500 V/20 A

3.2. BA

The BA was an optimization algorithm of swarm intelligence proposed by Professor Xin-She Yang in 2010 [21–23]. The algorithm was based on mimicking the echolocation of micro-bats in nature since the brain and neural system of hearing for a micro-bat could generate profound images of its surroundings by comparing between the pulses of the emitted sounds and the echoes that repetitively appeared. Therefore, most micro-bats could radiate sounds to the surrounding environment, where object size and distance were measured by listening to the echo of sounds from different objects. They could even measure the moving speed of objects and further identify prey locations, as well as evading obstructions or tracking in dark caves.

The iteration steps of the conventional BA were described as follows:

Step 1: Setting of the relevant parameters including the bat quantity (N), maximum iteration number (*Iter_max*), range of pulse frequency $[F_{min}, F_{max}]$ and maximum pulse rate r^m.
Step 2: Initialization of the parameters for each bat including the location x, pulse frequency F and flying speed v, while the iteration number was set as t = 0.
Step 3: Initialization of the values for each bat with the pulse emission rate r at 0 and loudness A between [0.5 and 1].
Step 4: Acquisition of the fitness value and recording of the optimal location x_{best} for each bat.
Step 5: Renewal of the iteration number $t = t + 1$ and generation of a random number "rand(•)".

In the case of rand(•) > r, Equation (2) was used to renew the location x_i^t of the bat i; conversely, Equations (3)–(5) were used for the pulse frequency F, location x and speed v of each bat.

$$x_i^t = x_i^{t-1} + \varepsilon A^t \tag{2}$$

$$F_i = F_{min} + \alpha(F_{max} - F_{min}) \tag{3}$$

$$v_i^t = v_i^{t-1} + F_i(x_i^t - x_{best}) \tag{4}$$

$$x_i^t = x_i^{t-1} + v_i^t \tag{5}$$

among them, ε was the random number between [–1 and 1], α was the random number between [0 and 1], A^t was average loudness of the swarm, and x_{best} was the optimal location at present.

Step 6: Use of Equations (6) and (7) to renew loudness A and pulse emission rate r for each bat.

$$A_i^{t+1} = \beta A_i^t \tag{6}$$

$$r_i^{t+1} = r^m[1 - \exp(-\gamma \times t)] \tag{7}$$

where β was the constant of normal distribution within [0, 1] and γ was the constant greater than zero.

Step 7: Renewal for optimal location and fitness value.

Step 8: Should the iteration number reach the preset maximum iteration number, the iteration was stopped and the optimal location x_{best} at present was produced. Conversely, should the iteration number failed to reach the maximum iteration number set, the process returned to Step 5.

4. IIBA Proposed for MPPT

In the case of the conventional BA with a PVMA under shading of different parts, although the GMPP could be tracked, the tracking direction was determined by random number, which led to the need of a longer duration for the algorithm to track the true MPP and resulted in a poor dynamic response. Because the size of the tracking pace was also determined by random number, the output power of a PVMA would oscillate nearby when the output power was close to the GMPP. This caused power loss and further reduced the power generation efficiency.

4.1. BA Pacing Adjustment with Gradient in P-V Curve

To solve the problem of poor performance in dynamic and steady responses with the conventional BA, the IIBA proposed in this paper adjusted the tracking direction and pacing magnitude with the gradient of the P-V curve. Firstly, the output voltage and power of a PVMA were read, where the two parameters were used for calculating the gradient of the P-V curve (shown as Equation (8)). Subsequently, the location of the bat swarm was renewed according to Equation (9).

$$m_i^t = \frac{P_i^t - P_i^{t-1}}{V_i^t - V_i^{t-1}} \tag{8}$$

$$x_i^t = x_i^{t-1} + \varepsilon \times m_i^t \tag{9}$$

Since the conventional BA mainly renewed locations with loudness A, and such loudness A was limited to parameters between [0 and 1], should the gradient of the P-V curve range too wide, there would be a scattering problem during the tracking process. To solve such a problem, the range of ε set values were to be narrowed.

4.2. Pacing Adjustment and Fixed Initial Tracking Voltage with Gradient of P-V Curve

Due to the excessively long tracking duration and greater oscillation during tracking for the conventional BA, the modified BA proposed in this paper adjusted the tracking paces with the gradient of the P-V curve. Therefore, compared to the conventional BA that could shorten the duration of the GMPP tracking and improve the problem of excessive oscillations from tracking to the MPP vicinity, the BA proposed in this paper, for the sake of reducing the tracking time and increasing the power generation efficiency, besides adjusting the tracking paces with the gradient of the P-V curve, the initial tracking voltage V_{st} was set as 0.8 times that of the MPP voltage V_{mp} for a PVMA under STCs, i.e., $V_{\mathrm{st}} = 0.8\ V_{\mathrm{mp}}$. The improvement method proposed only required adjustment on one iteration step in the conventional BA to shorten the tracking time, which further enhanced the efficiency of the photovoltaic system. Figure 5 displays the flow chart of the IIBA proposed in this paper.

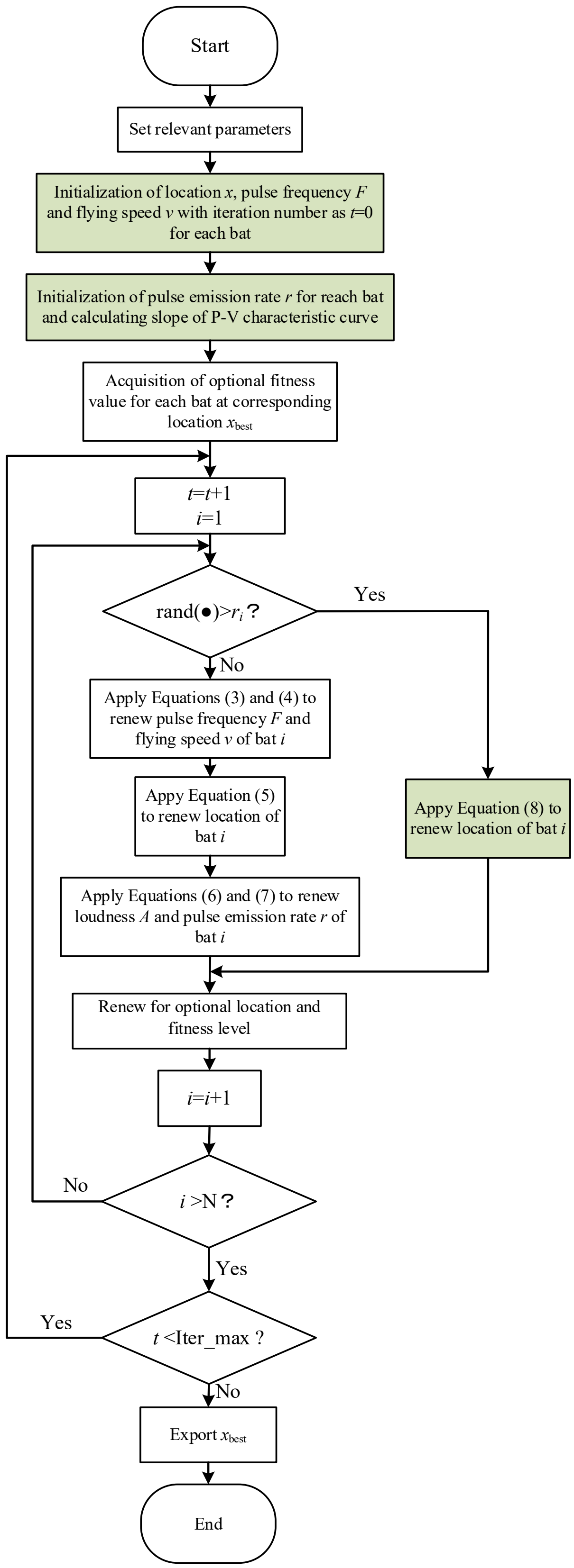

Figure 5. Flow chart of IIBA proposed in this paper.

5. Simulation Results

In this paper, MATLAB/Simulink was utilized to build the MPPT system for a PVMA, so the tracking results of the MPPT method proposed could be simulated. During the simulation, the solar irradiance of 12 photovoltaic modules was simultaneously reduced by half at 0.4 s. However, the shading percentage stayed the same to test that under the scenario of a sudden weather change, the output power (P_{pv}) of a PVMA under the IIBA proposed could still work at the GMPP instead of the LMPP. The conditions of shaded percentage set during test are shown in Table 3, while Table 4 displays the parameters used for the conventional BA and IIBA. For easier comparison between the three types of BA regarding the effect of application on the MPPT for a PVMA, each iteration renewal of these three methods in this paper was set with the same delay time to prolong the actual tracking time.

Table 3. Peak numbers appeared in P-V curve for 4-Series–3-Parallel PVMA under different shading.

Case	Peak Number in P-V Curve	4-Series-3-Parallel Shade %
1	1 peak	(0% shade +0% shade +0% shade +0% shade)// (0% shade +0% shade +0% shade +0% shade)// (0% shade +0% shade +0% shade +0% shade)

2	2 peaks
	(MPP on right)
		(0% shade +40% shade +0% shade +0% shade)//
		(0% shade +0% shade +0% shade +0% shade)//
		(0% shade +0% shade +0% shade +0% shade)

3	3 peaks (MPP on left)	(0% shade +70% shade +50% shade +0% shade)// (0% shade +70% shade +50% shade +0% shade)// (0% shade +70% shade +50% shade +0% shade)

4	3 peaks
	(MPP at middle)
		(90% shade +0% shade +0% shade +30% shade)//
		(0% shade +0% shade +0% shade +0% shade)//
		(0% shade +0% shade +0% shade +0% shade)

5	4 peaks (MPP at second peak)	(0% shade +80% shade +50% shade +10% shade)// (0% shade +80% shade +50% shade +10% shade)// (0% shade +80% shade +50% shade +10% shade)

6	4 peaks
	(MPP on far right)
		(0% shade +80% shade +50% shade +20% shade)//
		(0% shade +0% shade +0% shade +0% shade)//
		(0% shade +0% shade +0% shade +0% shade)

Note: "+" represented series and "//" represented parallel.

Table 4. Parameters used in conventional BA and IIBA.

Name of Parameter	Conventional BA	Improved BA
Maximum iteration number (*Iter_max*)	100	100
The population size (N)	4	4
Range of pulse frequency [F_{min}, F_{max}]	[0.2, 0.8]	[0.2, 0.8]
Maximum pulse rate r^m	0.9	0.9
Initial pulse rate r	0	0
Initial loudness A	(0.5, 1]	A not used
ε range	[−1, 1]	[−0.25, 0]
α range	[−1, 1]	[−1, 1]
β	0.8	0.8
γ	0.9	0.9

(1) Test Results of Case 1

Figure 6a displays the P-V and I-V curves of a PVMA under STCs in Case 1, with no shading and MPP at 239.12 W. Figure 6b displays the P-V and I-V curves of a PVMA in Case 1, with no shading, solar irradiance at 500 W/m^2 and MPP at 121.07 W. Figure 7 displays the simulation results of MPPT from using the conventional BA, the IIBA under pacing adjustment with the gradient of the P-V curve, and the IIBA under simultaneous pacing adjustment with the gradient of the P-V curve and the fixed initial tracking voltage at $V_{\mathrm{st}} = 0.8\ V_{\mathrm{mp}}$. From the simulation results, it can be known that all three methods could track the GMPP. However, the IIBA under simultaneous pacing adjustment with the gradient of the P-V curve and the fixed initial tracking voltage at 0.8 V_{mp} produced the fastest tracking for a dynamic response, and its steady responding performance was the best among the three methods.

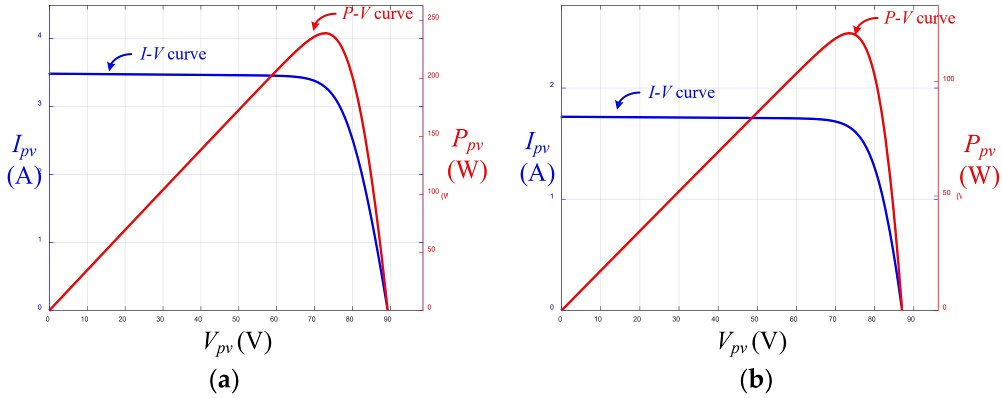

Figure 6. P-V and I-V curves of Case 1: (**a**) under STCs; (**b**) solar irradiance at 500 W/m^2.

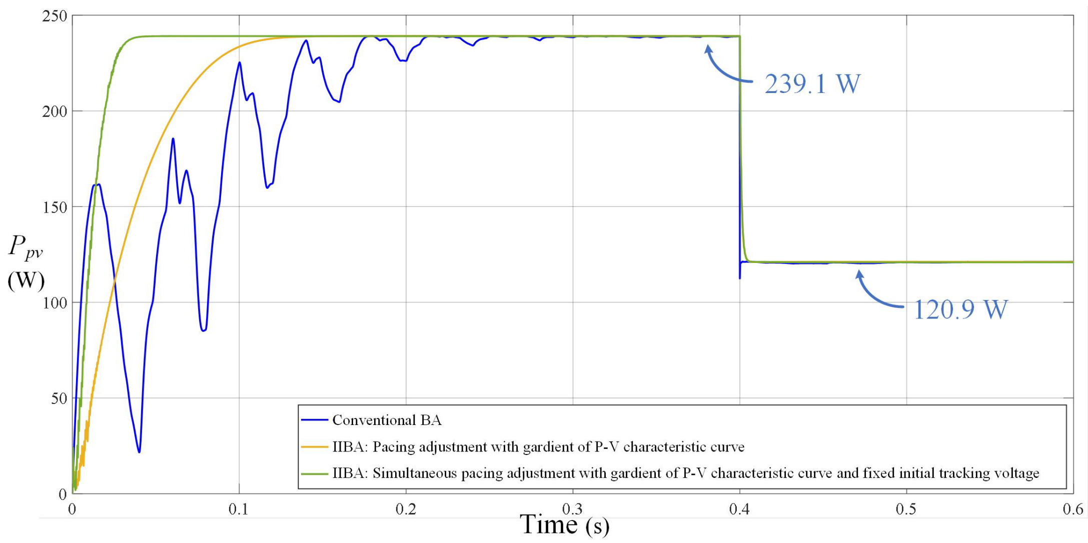

Figure 7. Simulation results of Case 1.

(2) Test Results of Case 2

Figure 8a displays the P-V and I-V curves of a PVMA under STCs in Case 2, with the location of a single module as shown in Table 3 under 40% shading, which presented 2-peak values with the GMPP at 210.13 W on right side. Figure 8b displays the P-V and I-V curves of a PVMA in Case 2, with a single module under the same shading percentage but solar irradiance at 500 W/m^2 and the GMPP at 106.38 W, also on right side. Figure 9 demonstrates the simulation results of MPPT when using the conventional BA, the IIBA under pacing adjustment with the gradient of P-V curve, and the IIBA under simultaneous pacing adjustment with the gradient of the P-V curve and the fixed initial tracking voltage at $V_{\rm st}$ = 0.8 $V_{\rm mp}$. From the simulation results, it can be known that all three methods could track the GMPP. However, the IIBA under simultaneous pacing adjustment with the gradient of the P-V curve and the fixed initial tracking voltage at 0.8 $V_{\rm mp}$ was faster to escape from the LMPP than the other two methods at 187 W, thus the GMPP at 210 W could be tracked in very short duration. In view of this, it could be distinctively known that tracking speed of such a method had the fastest dynamic response and steady performance among the three methods. Similarly, all three methods could track the new GMPP swiftly under the instant change of the solar irradiance to 500 W/m^2.

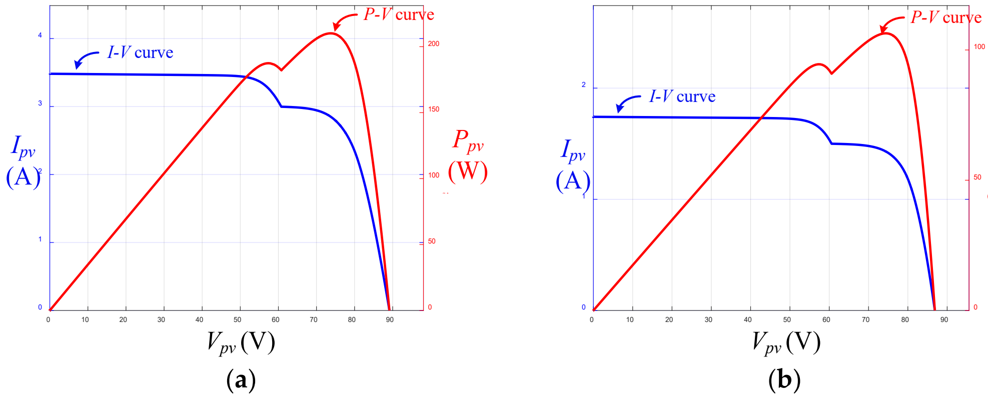

Figure 8. P-V and I-V curves of Case 2: (**a**) under STCs; (**b**) solar irradiance at 500 W/m^2.

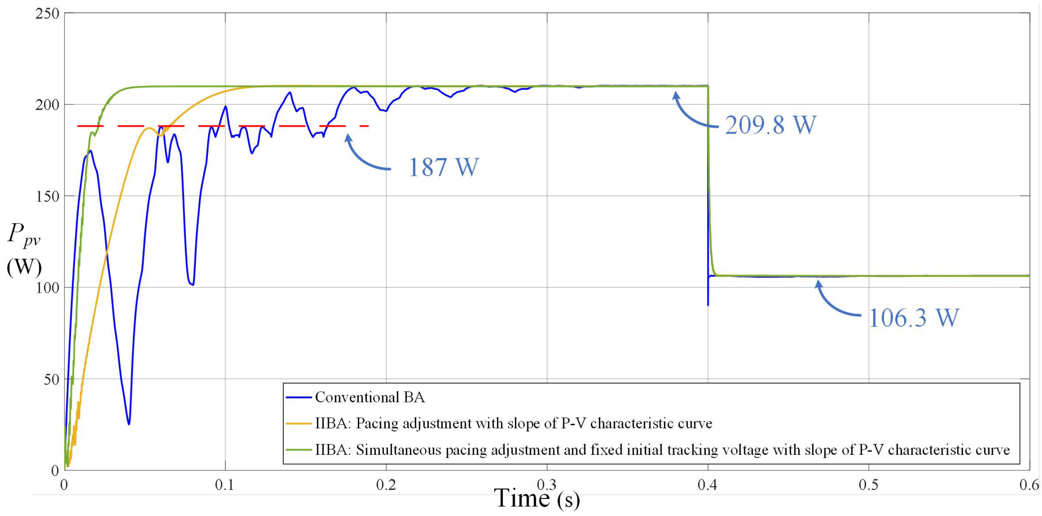

Figure 9. Simulation results of Case 2.

(3) Test Results of Case 3

Figure 10a displays the P-V and I-V curves of a PVMA under STCs in Case 3, with six modules as shown in Table 3 under 70% shade and 50% shade, which presented 3-peak values with the GMPP at 114.31 W on the far left. Figure 10b displays the P-V and I-V curves of a PVMA in Case 3, with six modules under the same shading but solar irradiance at 500 W/m^2 and GMPP at 57.95 W, also on the far left. Figure 11 demonstrates the simulation results of MPPT from using the traditional BA, the IIBA under pacing adjustment with the gradient of the P-V curve, and the IIBA under simultaneous pacing adjustment with the gradient of the P-V curve and the fixed initial tracking voltage at 0.8 V_{mp}. From the simulation results, it can be known that all three methods could track the GMPP at 114.1 W. Although the conventional BA could track the MPPT swiftly with solar irradiance at 500 W/m^2, the large oscillation during tracking could not be prevented, where steady work near the location was not feasible even when the true MPP was tracked. However, the IIBA under pacing adjustment with the gradient of the P-V curve was faster than conventional methods during MPPT, and the GMPP could be tracked steadily. As for the IIBA under simultaneous pacing adjustment with the gradient of the P-V curve and the fixed initial tracking voltage at 0.8 V_{mp}, it had the fastest dynamic response and best performance of steady response among the three methods.

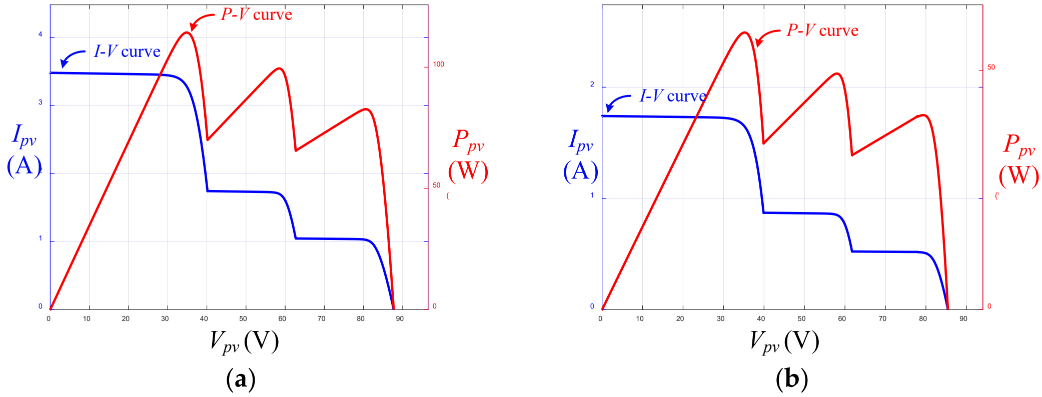

Figure 10. P-V and I-V curves of Case 3: (**a**) under STCs; (**b**) solar irradiance at 500 W/m^2.

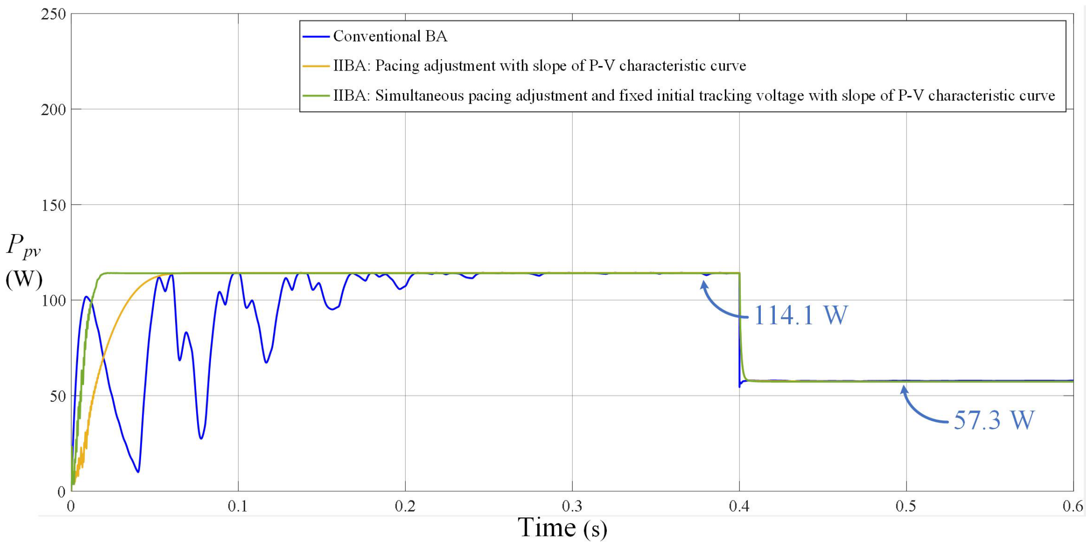

Figure 11. Simulation results of Case 3.

(4) *Test Results of Case 4*

Figure 12a displays the P-V and I-V curves of a PVMA under STCs in Case 4, with the location of the two modules as shown in Table 3 under 90% shade and 30% shade. The P-V curves presented 3-peak values with the GMPP at 178.93 W at the middle location. Figure 12b displays the P-V and I-V curves of a PVMA in Case 4, with the two modules under the same shading but the solar irradiance at 500 W/m^2 and the GMPP at 89.42 W, also at the middle location. Figure 13 demonstrates the simulation results of MPPT from using the traditional BA, the IIBA under pacing adjustment with the gradient of the P-V curve, and the IIBA under simultaneous pacing adjustment with the gradient of the P-V curve and the fixed initial tracking voltage at 0.8 V_{mp}. From the simulation results, it can be known that all three methods could track the GMPP at 178.6 W under STCs and 89.3 W when solar irradiance changed to 500 W/m^2. From Figure 13, it can be observed that the IIBA under simultaneous pacing adjustment and the fixed initial tracking voltage at 0.8 V_{mp} with the gradient of the P-V curve was distinctively faster to escape from the LMPP than the other two algorithms at 121.5 W, as well as swiftly tracking to the GMPP and maintaining the MPP for a PVMA steadily. Moreover, it can also be observed from Figure 13 that all three methods were not stuck at the first local peak value under 61.37 W when the solar irradiance changed to 500 W/m^2. Since the voltage location of the GMPP under STCs was fairly close to the location of the GMPP when the solar irradiance changed to 500 W/m^2, all three methods could track the new GMPP immediately. However, the IIBA under pacing adjustment with the gradient of the P-V curve had a slight oscillation nearby when tracking to the GMPP. Therefore, this case displayed that the IIBA under simultaneous pacing adjustment with the gradient of the P-V curve and the fixed initial tracking voltage at 0.8 V_{mp} can achieve better performances for the dynamic response and steady response.

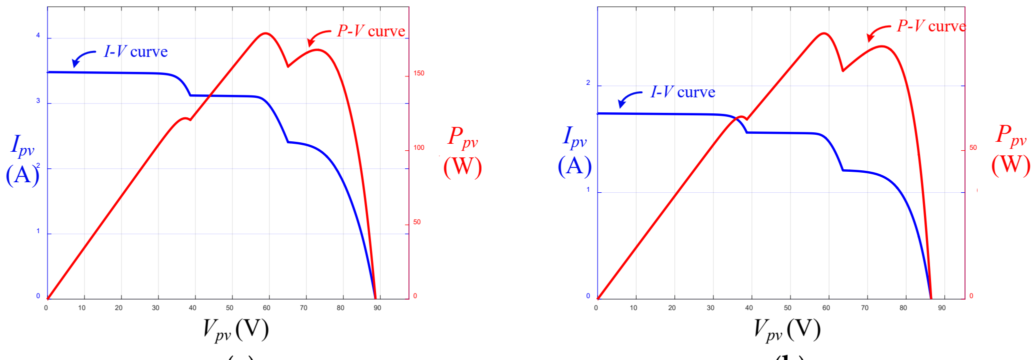

Figure 12. P-V and I-V curves of Case 4: (**a**) under STCs; (**b**) solar irradiance at 500 W/m^2.

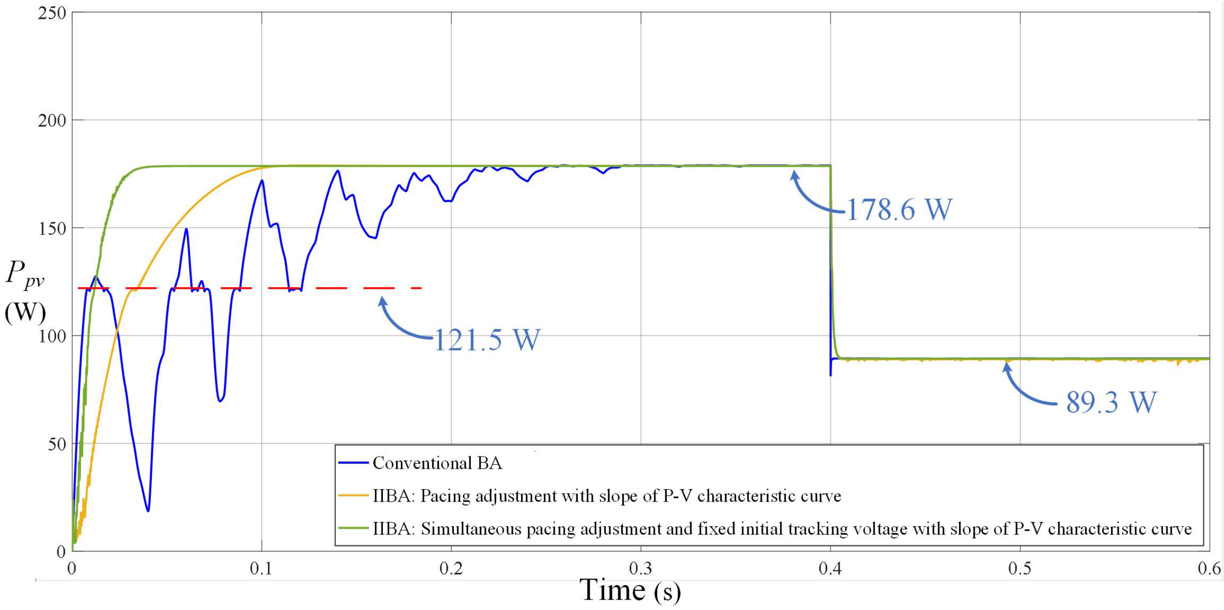

Figure 13. Simulation results of Case 4.

(5) Test Results of Case 5

Figure 14a displays the P-V and I-V curves of a PVMA under STCs in Case 5, with nine modules as shown in Table 3 under 80% shade, 50% shade and 10% shade, which presented 4-peak values with the GMPP under the output power of 106.64 W on the second peak. Figure 14b displays the P-V and I-V curves of a PVMA in Case 5, with nine modules under the same shading but the solar irradiance at 500 W/m^2 and the GMPP at 53.85 W, also on the second peak. Figure 15 demonstrates the simulation results of MPPT from using the conventional BA, the IIBA under pacing adjustment with the gradient of the P-V curve, and the IIBA under simultaneous pacing adjustment with the gradient of the P-V curve and the fixed initial tracking voltage at 0.8 V_{mp}. From the simulation results, it can be known that all three methods can track the true GMPP at 106.6 W and 53.8 W under STCs and when the solar irradiance changed to 500 W/m^2. The conventional BA faced the same problem of being stuck at the LMPP of 51.5 W and failed to escape instantly, which led to a longer duration for tracking to the GMPP and excessive oscillations near the MPP. The IIBA under pacing adjustment with the gradient of the P-V curve and the IIBA under simultaneous pacing adjustment with the gradient of the P-V curve and the fixed initial tracking voltage at 0.8 V_{mp} would be stuck at the LMPP for a shorter duration and escape rapidly but track the GMPP swiftly. From the simulation results, it can be distinctively observed that the IIBA under simultaneous pacing adjustment with the gradient of the P-V curve and the fixed initial tracking voltage at 0.8 V_{mp} had the fastest dynamic response and best performance of steady response among the three methods.

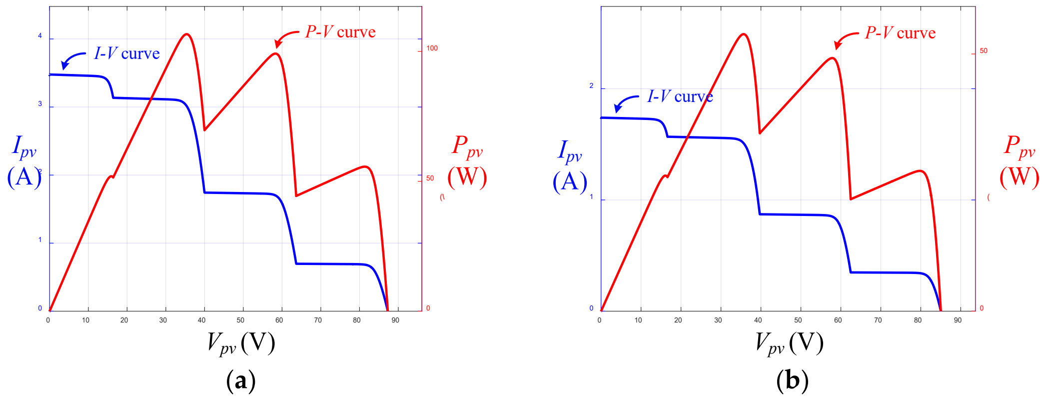

Figure 14. P-V and I-V curves of Case 5: (**a**) under STCs; (**b**) solar irradiance at 500 W/m^2.

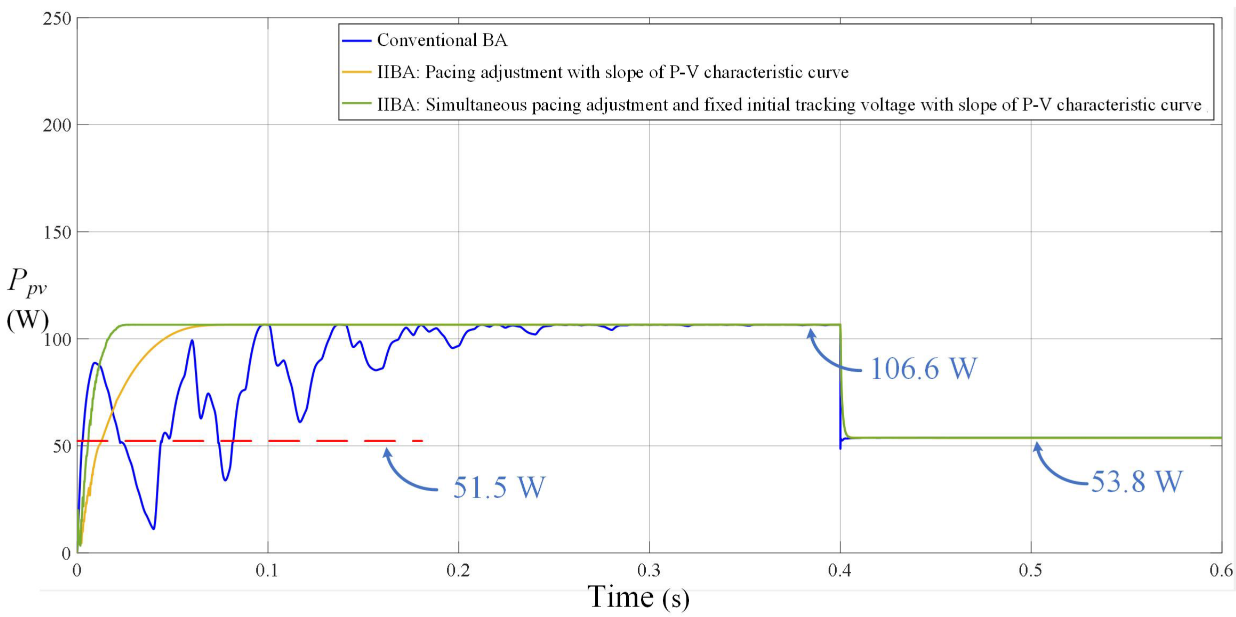

Figure 15. Simulation results of Case 5.

(6) Test Results of Case 6

Figure 16a displays the P-V and I-V curves of a PVMA under STCs in Case 6, with three modules as shown in Table 3 under 80% shade, 50% shade and 20% shade, which presented 4-peak values with the GMPP under an output power of 176.28 W on the far right. Figure 16b displays the P-V and I-V curves of a PVMA in Case 6, with three modules under the same shading but the solar irradiance at 500 W/m^2 and the GMPP at 89.29 W, also on the far right. Figure 17 demonstrates the simulation results of MPPT from using the traditional BA, the IIBA under pacing adjustment with the gradient of the P-V curve, and the IIBA under simultaneous pacing adjustment with the gradient of the P-V curve and the fixed initial tracking voltage at 0.8 V_{mp}. From the simulation results, it can be observed that all three methods could track the GMPP. Compared to the other two methods, the IIBA under simultaneous pacing adjustment with the gradient of the P-V curve and the fixed initial tracking voltage at 0.8 $V_{mp,}$ can escape three LMPPs, namely the MPP of 53.5 W as the first peak value in P-V curve, the MPP of 117.0 W as the second peak value and the MPP of 169.1 W as the third peak value, where the GMPP was then tracked swiftly. Furthermore, this IIBA also had the best performance of tracking the steady response among the three methods.

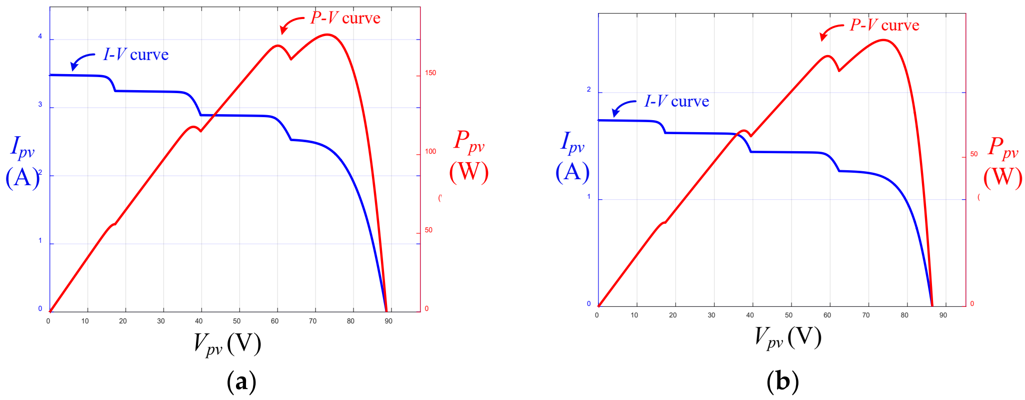

Figure 16. P-V and I-V curves of Case 6: (**a**) under STCs; (**b**) solar irradiance at 500 W/m^2.

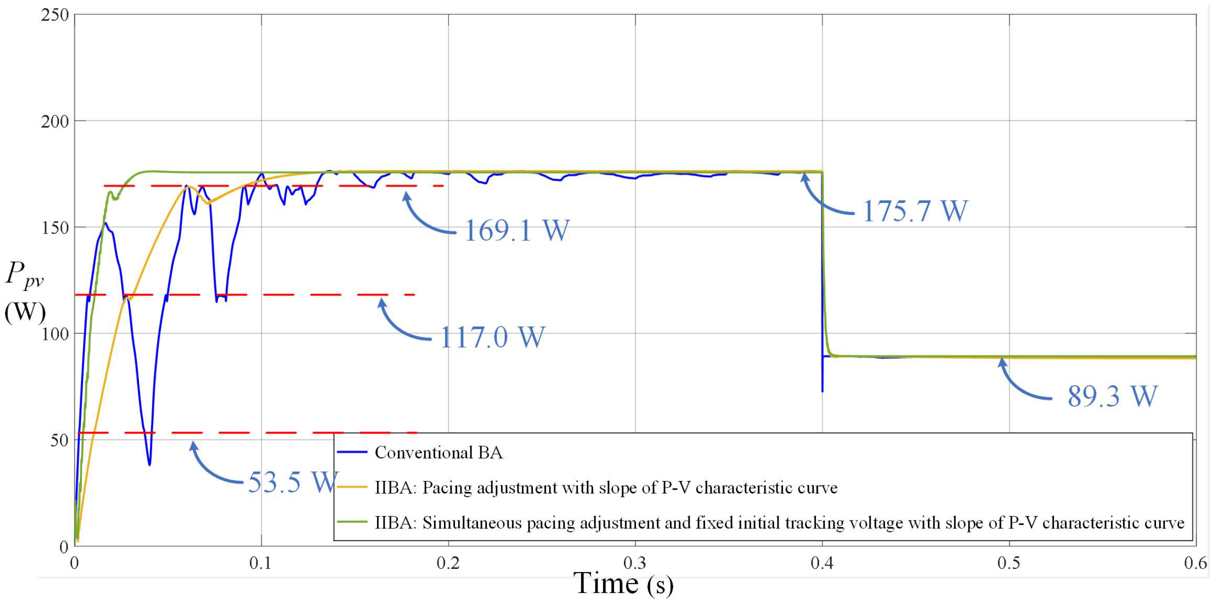

Figure 17. Simulation results of Case 6.

This article provides a detailed description of the necessary module specifications in Table 2, the parameters that the algorithms use in Table 4, and the shading ratios of the modules for each of the six different test case types in Table 3. In addition, simulation results in Table 5 discuss the requirements for quantifying tracking using various intelligent maximum tracking point tracking techniques.

Table 6 demonstrates that the two proposed types of improved intelligent bat algorithms (IIBAs) outperform the improved firefly algorithm (IFA) [25] and the modified gray wolf optimization algorithm (MGWOA) [20] in terms of dynamic tracking speed and steady-state response.

Table 5. Comparison of simulation results for the six selected cases using various intelligent BAs.

Case	Number of Peak(s) of the P-V Curve	Conventional BA		IIBA under Pacing Adjustment with Gradient of P-V Curve		IIBA under Simultaneous Pacing Adjustment with Gradient of P-V Curve and Fixed Initial Tracking Voltage at 0.8 V_{mp}	
		Average Tracking Time	Average Maximum Power	Average Tracking Time	Average Maximum Power	Average Tracking Time	Average Maximum Power
1	1	0.22 s	239.51 W	0.13 s	238.72 W	0.04 s	238.92 W
2	2	0.25 s	209.84 W	0.12 s	210.08 W	0.04 s	209.95 W
3	3	0.21 s	114.09 W	0.06 s	114.02 W	0.02 s	114.14 W
4	3	0.22 s	177.94 W	0.11 s	178.50 W	0.03 s	178.52 W
5	4	0.21 s	106.57 W	0.07 s	106.39 W	0.02 s	106.58 W
6	4	0.23 s	175.69 W	0.13 s	175.60 W	0.04 s	176.11 W

Table 6. Comparison of simulation results for the six selected cases with different intelligent MPPT methods.

Case	Number of Peak(s) of the P-V Curve	Method Proposed in [25]		Method proposed in [20]		IIBA under Pacing Adjustment with Gradient of P-V Curve		IIBA under Simultaneous Pacing Adjustment with Gradient of P-V Curve and Fixed Initial Tracking Voltage at 0.8 V_{mp}	
		Average Tracking Time	Average Maximum Power	Average Tracking Time	Average Maximum Power	Average Tracking Time	Average Maximum Power	Average Tracking Time	Average Maximum Power
1	1	0.7 s	244.5 W	0.5 s	244.5 W	0.13 s	238.72 W	0.04 s	238.92 W
2	2	1.0 s	211.2 W	0.9 s	211.2 W	0.12 s	210.08 W	0.04 s	209.95 W
3	3	1.4 s	124.9 W	1.5 s	124.9 W	0.06 s	114.02 W	0.02 s	114.14 W
4	3	1.3 s	183.9 W	0.9 s	183.9 W	0.11 s	178.50 W	0.03 s	178.52 W
5	4	2.0 s	114.0 W	2.4 s	114.0 W	0.07 s	106.39 W	0.02 s	106.58 W
6	4	1.7 s	192.0 W	2.2 s	192.0 W	0.13 s	175.60 W	0.04 s	176.11 W

6. Conclusions

There are currently no documented cases of using the bat algorithm in a photovoltaic module array to track the maximum power point. In light of this, in this study, traditional bat algorithms are applied to the photovoltaic array to carry out maximum power point tracking, but they are further improved so that they not only increase tracking speed but also do not fall into the local maximum power point, thus simultaneously improving dynamic tracking response and steady-state performance. Furthermore, the simulation results present that the two types of improved intelligent bat algorithm (IIBA) outperform the existing improved firefly algorithm (IFA) and modified gray wolf optimization algorithm (MGWOA) in dynamic tracking speed and steady-state response. In this paper, two IIBAs were proposed for MPPT of a PVMA under different shaded conditions and different solar irradiance, which could enhance the tracking efficiency, improve the power generation benefits and reduce the energy loss. By adjusting the tracking pace of the conventional BA according to the gradient of the P-V curve, the initial tracking voltage was simultaneously set at 0.8 times (i.e., V_{st} = 0.8 V_{mp}) the maximum power of a PVMA under STCs. Moreover, the MATLAB/Simulink software was adopted to simulate applications in a PVMA under different shaded conditions, where MPPT was conducted when multiple peak values occurred in the P-V curves. The two IIBAs proposed in this paper were the IIBA under pacing adjustment with the gradient of the P-V curve and the IIBA under simultaneous pacing adjustment with the gradient of the P-V curve and the fixed initial tracking voltage at 0.8 V_{mp}. Among them, the IIBA under simultaneous pacing adjustment with the gradient of the P-V curve and the fixed initial tracking voltage at 0.8 V_{mp} could swiftly escape from the LMPP and correctly track the GMPP, which had the optimal tracking performance for dynamic response and steady response. Compared to the conventional BA, the IIBA proposed did not only have better speed in tracking response, but it could also reduce the power loss during the tracking process, which further enhanced the power generation efficiency. From the simulation results, it was demonstrated that in the case of a PVMA under different shading scenarios and a sudden change in solar irradiance during tracking, the MPPT conducted with the IIBA proposed could provide better tracking performance in both the dynamic response and steady response. The improved bat algorithms proposed in this paper can be used to track the maximum power point in a photovoltaic module array (PVMA). Regardless of how many modules are subjected to different shading ratios, resulting in multiple peaks on the P-V curve, the global maximum power point can be quickly tracked. Simultaneously, the new global maximum power point can be accurately and quickly tracked as sunlight conditions change in real time. Currently, the completed simulation results prove the feasibility of the proposed improved bat algorithm, which is used in photovoltaic module arrays to track the global maximum power point. The future research direction is to apply it to an actual photovoltaic power generation site to track the global maximum point and further validate its tracking performance.

Author Contributions: K.-H.C. managed the project and completed the circuit design of the PV module simulator. K.-H.C. also planned the project and wrote, edited and reviewed the manuscript. T.T.T.B. completed the formal analysis of the maximum power point tracking algorithm. T.T.T.B. was also responsible for the software program and validation of the simulation results. All authors have read and agreed to the published version of the manuscript.

Funding: The authors gratefully acknowledge the support and funding of this project by the National Science and Technology Council, Taiwan, under the Grant Number NSTC 112-2221-E-167-002.

Institutional Review Board Statement: Not applicable.

Informed Consent Statement: Not applicable.

Data Availability Statement: Data are contained within the article.

Conflicts of Interest: The authors of the manuscript declare no conflicts of interest.

Nomenclature

Acronyms	
IIBA	improved intelligent bat algorithm
MPPT	maximum power point tracking
PVMA	photovoltaic module array
P-V	power–voltage
I-V	current–voltage
MPP	maximum power point
LMPP	local maximum power point
GMPP	global maximum power point
BA	bat algorithm
STCs	standard test conditions
P&O	perturbation and observation
INC	incremental conductance
CSA	cuckoo search algorithm
CSO	cat swarm optimization
GA	genetic algorithm
TLBO	teaching–learning-based optimization
AM	air mass
DSP	digital signal processor
PWM	pulse width modulation
Symbols	
V_{oc}	voltage of open circuit for photovoltaic
I_{sc}	current of short circuit for photovoltaic

V_{mp}	voltage of maximum power point for photovoltaic
I_{mp}	current of maximum power point for photovoltaic
P_{mp}	power at maximum power point for photovoltaic
T	the switching period of converter
D	duty cycle between [0 and 1]
V_{o}	the output voltage of boost converter
V_s	the input voltage of boost converter
t_{on}	the switch conduction time within one cycle
N	the population size
Iter_max	maximum iteration number
F_{min}	minimum of pulse frequency
F_{max}	maximum of pulse frequency
r^m	maximum pulse rate
x_{best}	optimal location at present
P_i	fitness value of bat i
t	the iteration number at present (t = 0 . . . *Iter_max*)
x_i^t	location of bat i of iteration t
v_i^t	flying speed of bat i of iteration t
F_i	pulse frequency of bat i
ε	random number between [−1 and 1] in BA; between [−0.25 and 0] in IIBA
α	random number between [0 and 1]
A^t	average loudness of the swarm
A_i^t	loudness of bat i of iteration t
r_i^{t+1}	pulse emission rate of bat i at iteration $t + 1$
γ	constant greater than zero
β	constant of normal distribution within [0, 1]
m_i^t	the gradient of P-V curve at present
P_i^t	power of photovoltaic at present
V_i^t	voltage of photovoltaic at present
V_{st}	initial tracking voltage
P_{pv}	the output power of a PVMA
V_{pv}	the output voltage of a PVMA
I_{pv}	the output current of a PVMA

References

1. Ghosh, S.; Alhatlani, A.; Safayatullah, M.; Batarseh, I. Review of MPPT Methods for LLC Converters in Photovoltaic Applications. In Proceedings of the 2022 IEEE Energy Conversion Congress and Exposition (ECCE), Detroit, MI, USA, 9–13 October 2022; pp. 1–6.
2. Routray, D.; Rout, P.K.; Sahu, B.K. A brief review and comparative analysis of two classical MPPT techniques. In Proceedings of the 2021 International Conference in Advances in Power, Signal, and Information Technology (APSIT), Bhubaneswar, India, 8–10 October 2021; pp. 1–6.
3. Ostadrahimi, A.; Mahmoud, Y. Curve Computation MPPT Method Based on Simple Modeling of the Photovoltaic Modules. In Proceedings of the 2020 International Conference on Smart Grids and Energy Systems (SGES), Perth, Australia, 23–26 November 2020; pp. 819–825.
4. Pawar, A.S.; Kolte, M.T.; Mehta, H. Review of PV MPPT Based Battery Charging Techniques under Partial Shading Conditions. In Proceedings of the 2022 Second International Conference on Power, Control and Computing Technologies (ICPC2T), Raipur, India, 1–3 March 2022; pp. 1–6.
5. Masoum, M.A.S.; Dehbonei, H.; Fuchs, E.F. Theoretical and experimental analyses of photovoltaic systems with voltage and current-based maximum power point tracking. *IEEE Tran. Energy Conv.* **2004**, *19*, 652–653. [CrossRef]
6. Yusong, Y.; Solomin, E.; Lei, W. Horizontal Axis Wind Turbine MPPT Control Research. In Proceedings of the 2020 International Conference on Industrial Engineering, Applications and Manufacturing (ICIEAM), Sochi, Russia, 18–22 May 2020; pp. 1–6.
7. Salem, M.H.; Bensalem, Y.; Abdelkrim, M.N. MPPT based on P&O control and FLC-Hill Climbing technique for a Photovoltaic Generator. In Proceedings of the 2021 18th International Multi-Conference on Systems, Signals & Devices (SSD), Monastir, Tunisia, 22–25 March 2021; pp. 589–594.
8. Goswami, Y.; Rana, K.P.S.; Kumar, V. Performance Analysis of an Improved Variable Step-Size IC MPPT Technique for SPV System. In Proceedings of the 2021 International Conference on Computing, Communication, and Intelligent Systems (ICCCIS), Greater Noida, India, 19–20 February 2021; pp. 822–827.

9. Anand, R.; Swaroop, D.; Kumar, B. Global Maximum Power Point Tracking for PV Array under Partial Shading using Cuckoo Search. In Proceedings of the 2020 IEEE 9th Power India International Conference (PIICON), Sonepat, India, 28 February–1 March 2020; pp. 1–6.
10. Li, M.; Liu, D.; Wang, C. Analysis of Photovoltaic Cell Power Characteristics Based on Cuckoo Search Algorithm. In Proceedings of the 2023 IEEE 5th International Conference on Power, Intelligent Computing and Systems (ICPICS), Shenyang, China, 14–16 July 2023; pp. 114–118.
11. Brindha, R.; Christy, A.A.; Anjaneya; Kumar, P.; Sarkar, A. Photovoltaic based Brushless DC Motor Using Cuckoo Algorithm as a Maximum Power Point Tracking. In Proceedings of the 2020 International Conference on Computational Intelligence for Smart Power System and Sustainable Energy (CISPSSE), Keonjhar, India, 29–31 July 2020; pp. 1–6.
12. Thangam, T.; Mythuvel, K. Hybrid Algorithm based PFoPID Control Design of a Grid-connected PV Inverter for MPPT. In Proceedings of the 2020 Second International Conference on Inventive Research in Computing Applications (ICIRCA), Coimbatore, India, 15–17 July 2020; pp. 992–998.
13. Xiu-cai, G.; Dan, X. Application of Improved Cat Swarm Optimization in MPPT Control of Photovoltaic Arrays. *IOP Conf. Ser. Earth Environ. Sci.* **2018**, *153*, 032024. [CrossRef]
14. Zhao, M.; Pan, J.S.; Chen, S.T. *Compact Cat Swarm Optimization Algorithm*; Springer: Cham, Switzerland, 2018; Volume 733, pp. 33–43.
15. Wu, Z.; Meng, R.; Cao, R. Research on Multi-peak MPPT of Photovoltaic Array Based on Quantum Genetic Algorithm. In Proceedings of the 2021 IEEE 5th Conference on Energy Internet and Energy System Integration (EI2), Taiyuan, China, 22–24 October 2021; pp. 392–396.
16. Mallat, M.; Kechiche, O.B.H.B.; Ezzeddine, K.; Hamouda, M. AN Optimized Genetic Algorithm (GA)-Based MPPT for Off-Grid Solar Photovoltaic System. In Proceedings of the 2023 IEEE International Conference on Artificial Intelligence & Green Energy (ICAIGE), Sousse, Tunisia, 12–14 October 2023; pp. 1–5.
17. Debbabi, F.; Mehazzem, F.; Soubdhan, T. Genetic Algorithm-based MPPT for Wind Power Conversion System: Study and Comparison with Conventional Method in Tropical Climate. In Proceedings of the 2023 5th Global Power, Energy and Communication Conference (GPECOM), Nevsehir, Turkiye, 14–16 June 2023; pp. 218–224.
18. Tehrani, V.M.; Rajaei, A.; Loghavi, M.A. MPPT Controller Design Using TLBO Algorithm for Photovoltaic Systems under Partial Shading Conditions. In Proceedings of the 2021 12th Power Electronics, Drive Systems, and Technologies Conference (PEDSTC), Drive Systems, Tabriz, Iran, 2–4 February 2021; pp. 1–5.
19. Millah, I.S.; Chang, P.C.; Teshome, D.F.; Subroto, R.K.; Lian, K.L.; Lin, J. An Enhanced Grey Wolf Optimization Algorithm for Photovoltaic Maximum Power Point Tracking Control under Partial Shading Conditions. *IEEE J. Ind. Electron. Soc.* **2022**, *3*, 392–408. [CrossRef]
20. Huang, K.-H.; Chao, K.-H.; Kuo, Y.-P.; Chen, H.-H. Maximum Power Point Tracking of Photovoltaic Module Arrays Based on a Modified Gray Wolf Optimization Algorithm. *Energies* **2023**, *16*, 4329. [CrossRef]
21. Eltamaly, A.M.; AI-Saud, M.S.; Abokhalil, A.G. A Novel Bat Algorithm Strategy for Maximum Power Point Tracker of Photovoltaic Energy Systems under Dynamic Partial Shading. *IEEE Access* **2020**, *8*, 10048–10060. [CrossRef]
22. Amalo, K.A.; Birninkudu, S.I.; Bukata, B.B.; Salawudeen, A.T.; Ahmad, A.A. Cultured Bat Algorithm for Optimized MPPT Tracking Under Different Shading Conditions. In Proceedings of the 2020 International Conference in Mathematics, Computer Engineering and Computer Science (ICMCECS), Ayobo, Nigeria, 18–21 March 2020; pp. 1–8.
23. Pervez, I.; Antoniadis, C.; Ghazzai, H.; Massoud, Y. A Modified Bat Algorithm with Reduced Search Space Exploration for MPPT under Dynamic Partial Shading Conditions. In Proceedings of the 2023 IEEE International Symposium on Circuits and Systems (ISCAS), Monterey, CA, USA, 21–25 May 2023; pp. 1–6.
24. Chao, K.-H.; Li, J.-Y. Global Maximum Power Point Tracking of Photovoltaic Module Arrays Based on Improved Artificial Bee Colony Algorithm. *Electronics* **2022**, *11*, 1572. [CrossRef]
25. Chao, K.-H.; Zhang, S.-W. An Maximum Power Point Tracker of Photovoltaic Module Arrays Based on Improved Firefly Algorithm. *Sustainability* **2023**, *15*, 8550. [CrossRef]
26. Szemes, P.T.; Melhem, M. Analyzing and modeling PV with "P&O" MPPT Algorithm by MATLAB/SIMULINK. In Proceedings of the 2020 3rd International Symposium on Small-Scale Intelligent Manufacturing Systems (SIMS), Gjovik, Norway, 10–12 June 2020; pp. 1–6.
27. Soumana, R.A.; Saulo, M.J.; Muriithi, C.M. Comparison of MPPT Techniques on THD Current in a Grid-Connected Photovoltaic System. In Proceedings of the 2022 4th Global Power, Energy and Communication Conference (GPECOM), Nevsehir, Turkey, 14–17 June 2022; pp. 95–100.
28. SunWorld Datasheet. Available online: http://www.ecosolarpanel.com/ecosovhu/products/18569387_0_0_1.html (accessed on 1 September 2022).
29. Hart, D.W. *Introduction to Power Electronics*, 2nd ed.; Pearson Education Taiwan Ltd.: Taipei, Taiwan, 2002; pp. 211–220.